Seismicity and seismotectonics study in Southwestern Albania using a local dense seismic network

A. Serpetsidaki, G-A. Tselentis, N. Martakis and E. Sokos

Keywords, microearthquakes, focal mechanism, stress inversion, seismotectonics

Abstract

The Albanides represent a complex orogen made up of a heterogeneous tectonic nappe pile of Paleozoic, Mesozoic and Cenozoic domains. Albania is tectonically active and moderate to strong earthquakes have occurred in the past. However, abundant microseismicity has not been monitored and studied by a dense seismic network. During this study a seismic network of 40 stations was deployed in southern Albania for one year. A total of 2113 microearthquakes were well located. The most accurately located events and 810 focal mechanisms were used in order to define the seismotectonics and the stress pattern in the area. Results indicate that thrust and strike-slip faulting both exist in southwestern Albania suggesting a continuation of the complex tectonic setting of the neighboring northwestern Greece to the north.

Introduction

Albania is one of the most earthquake-prone countries in the Mediterranean region, and is periodically subject to moderate to severe earthquake activity (Albania Ministry of Industry and Energy, 2003). The entire coastline of Albania lies on active fault zones and most earthquakes result from the periodic movement of blocks along the deep-seated Ionian-Adriatic faults. The country is characterized by intense microearthquake activity ($1.0<M<3.0$) and shallow crustal seismicity (Aliaj, 2007; Muco et al., 2002). The Albanian orogenic belt trends NNW-SSE and lies between the Dinaric and Hellenic Alps. The study area of this paper, geographically lies in southern Albania while geologically

belongs to Ionian isopic zone; more specific in Cika and Kurveleshi belts, which form an unbroken, elongated unit that extends continuously southwards into Greece (Robertson et al., 2001). According to the USGS database, which provides the seismicity since 1973, several, mainly moderate, seismic events are spread out in the study area, although the northern part of the region appears to be more active (Fig. 1).

Many towns and rural areas in Albania are seriously damaged from time to time by large and moderate earthquakes (Muco et al., 2002). According to the seismogenic models the study area lies in a zone, which is characterized by Mmax=7.0 (Aliaj, 2007). Consequently the information about active faulting is consummative in seismic hazard of the area. Moreover, as far as it concerns the southernmost Albania, in spite the complicated geotectonical regime, the knowledge comes mainly from the surface geology and well data in the area. Therefore, it is useful to study the area with a microearthquake network that records the intense microearthquake activity, since spatial distribution of microseismicity provides important information on fault structures.

Moreover, Albania is a country with proven oil and gas reservoirs and hydrocarbon exploration activities have taken place in the area. In 1918 the first oil exploration took place in Vlore area and in 1987 the Delvina oil field was discovered. The first gas discovery was in 1963 in Divjaka (National Agency of Natural Resources, 2007). The determination of the stress regime and the identification of active faults from the microearthquake study are of great importance for the future exploration of oil and gas reservoirs.

In this paper, we processed high quality seismological data observed from the temporary network and located 2113 events. We present the recorded seismicity and we used selected events in a local earthquake tomography study. Thus, we obtained a 3D crustal velocity model and relocated seismicity. These data were used in order to calculate accurate fault plane solutions. Finally the fault plane solutions were inverted for the determination of the stress distribution.

Tectonic setting

The study area is located in the Ionian-Adriatic thrust fault zone, which presents a NW to nearly NNW trend and consists mainly of pure compression active thrust faults; these faults are cut by strike–slip faults, trending NE and SE (Aliaj, 2007). Kilias et al. (2001) suggested oblique reverse and strike-slip faults, which are often associated with the thrusts. The study area (Cika and Kurveleshi belts) is dominated by large-scale linear folds, cut by major high-angle reverse faults (Robertson and Shallo, 2000).

Figure 1 shows the major structures in the study area. There are three large anticlinal chains in the area associated with a dominant top-to-the-SW sense of movement, which consist of asymmetric, overturned NW-SE-trending folds and thrusts (Kilias et al., 2001). To the west, the anticlinal chain Shendelli-Saranda-Ksamil appears in Saranda and south of Butrinti, where it gradually dips into Quaternary deposits (Meco and Aliaj, 2000). To the east, the Saranda anticline is bounded by the Vurgu syncline. The Fterra – Fittore

anticlinal chain outcrops in the northern and southern part of the study area; to the south it meets the smaller Kronje anticline. The Mali i Gjere anticlinal chain is bounded to the west by the Delvina depression and dominates the eastern part of the study area. Southwest of the Malet i Kurveleshi - Mali i Gjere anticlinal chain, the smaller Krongji-Livine anticline appears.

Numerous longitudinal tectonic faults are located in a relatively wide belt within the orogen. On the western front of the Cika belt, there is a regional overthrusting fault, the Middle Ionian thrust. The northern part deviates northeastward, cutting off the Cika and Kurveleshi belts. The Outer Ionian thrust limits the Mali i Gjere to the east and smaller faults move parts of the anticlines in vertical NE – SW direction.

The tectonic setting is strongly related to the upper-Triassic diapirism. The evaporites outcrop along regional tectonic faults (i.e. Glina) and local structures (Delvina, Fterra) (Velaj, 2001). Salts are widespread in the Kurveleshi belt (Rusani, Fterra, Picar-Kardhiqi), whereas gypsum and anhydritic facies dominate in the western Cika belt (Zhulati-Kardhiki, Glina, Xarra, Glifku, Navarica, Cerkavica) (Velaj, 1985).

Seismograph Network and Data

The study area is located in the south-southwestern part of Albania and spans 20x40 km^2. A temporary microearthquake network consisting of 40 EarthData PR24 stations supplemented with LandTech LT-S01 three component velocity sensors was deployed

from January 12th, 2008 to February 3rd, 2009, with an average spacing of 5 km (Fig.1). Station coordinates were established by differential GPS measurements with a horizontal accuracy of ±2 m and a vertical accuracy of ±1 m. The instruments have a flat transfer function for velocity in the frequency range 1 to 50 Hz. The recording was continuous with a sampling frequency of 100 Hz.

During the operation of the network, approximately 2500 teleseismic, regional and local events were recorded (Fig. 2). Many explosions from exploration fields in the area were also recorded. A total of 2113 events were located, of which 90% were located within the area covered by the microseismic network Most of the events are located by 10-30 picks (P and S wave arrivals), with a mean of 25 picks (Fig.3a). The mean RMS (Root Mean Square) travel time residual is 0.11 sec (Fig.3b), the mean ERH (Horizontal Error) is 0.4 km (Fig3c) and the mean ERZ (Vertical Error) is 0.5 km (Fig3d). The majority of the events are weak, with a duration magnitude ranging from M1 to M2; events weaker than M0.5 or greater than M3 were rare (Fig.3e). Most of the seismic events were shallower than 15 km, with a large number of the hypocenters concentrated at depths between 5 and 10 km.

Method

The first stage of data analysis process included an automatic search for seismic events in the dataset of each station. A program was developed, based on the STA/LTA (Short Term Average/ Long Term Average) algorithm (Korn and Korn, 1968), in order to

identify events and merge event files. In a next step, the selected events per station were crosschecked automatically, and in case an event was detected at more than six stations, it was triggered as a real event (otherwise as a false one). Finally, the P and S wave arrivals of the seismic events were manually picked using SEISMWIN software (Xanalatos and Tselentis, 1997).

The initial hypocentral locations were determined using HYPO71 program (Lee and Lahr, 1975, Lee and Valdes, 1985). The 1-D velocity model adopted for this procedure (Table 1) was proposed by Tselentis et al., 2006. This model is reliable and well tested from a previous passive seismic tomography survey in the adjacent area of Epirus in NW Greece. The study area is located within the same isopic zone (Ionian Zone), with similar geotectonic characteristics (King et al., 1983). Thus, this crustal model is appropriate for locating events in our case.

Furthermore, the most accurately located events (1859) were used in a 3D tomographic study. The tomographic inversion procedure was performed in two main steps. In the first step an optimum 1D P-wave velocity model was estimated, using the VELEST software (Kissling et al, 1994) for 1D joint hypocentral-velocity inversion. In this procedure the initial velocity model was the same as the one used in HYPO71 (Table 1). In the second step, the results of the previous stage were used as input for the 3D tomographic inversion. The software that was used for this purpose was an updated version of *Simulps12* (Thurber, 1986; Evans et al., 1994). The tomographic study and results are described in detail by Tselentis et al, 2011.

Finally, the fault plane solutions were determined using the FPFIT program (Reasenberg and Oppenheimer, 1985) with the events' azimuth and angle of incidence computed during the tomography inversion. For each fault-plane solution, FPFIT calculates several uncertainty indexes to characterize the quality of the final solution. Main indexes are the norm misfit function F_j ($F_j = 0.0$ represents a perfect fit) and the station distribution ratio ($0.0 \leq STDR \leq 1.0$). When the STDR has a low value (< 0.5), then a relatively large number of the data lie near nodal planes in the solution. Such a solution is less robust than the one with $STDR > 0.5$. The uncertainties in strike, dip and rake, ΔSTR, ΔDIP, ΔRAK of the final solutions should be smaller than 20° (Reasenberg and Oppenheimer, 1985).

Out of 2113 events, more than 1000 were located with 25 or more P-wave first arrivals and were selected as input to FPFIT. Only unique solutions were selected, resulting in a dataset of 810 reliable fault plane solutions and well-constrained nodal planes, with mean misfit function $F_{j,}$ equal to 0.19, mean STDR equal to 0.7 and errors in strike, dip and rake (ΔSTR, ΔDIP, ΔRAK) smaller than 10^o. The computed fault plane solutions were used for stress tensor inversion using the method of Gephart and Forsyth (Gephart and Forsyth, 1984; Gephart 1990).

Results and Discussions

1. Seismicity

The seismicity recorded during this study is shown in Figure 2a and is more concentrated in the northern part of the study area. The seismic events are concentrated in clusters, although some scattered epicenters also exist. The earthquakes are shallow, with hypocentral depths varying mainly from 1 to 10 km; earthquakes below 15 km are rare. The earthquake depth increases slightly to the East, while some clusters show concentrations in certain depths (Fig2b).

The results confirm that the area is characterized by intense microearthquake activity ($1.0<M<3.0$) and shallow crustal seismicity (Aliaj, 2007; Muco et al., 2002). The shallow seismicity is related to the continental collision, which creates a series of NW-SE thrusts fronts involving the Apulian platform itself (Tiberti et al., 2008). Seismic profiles image the sole-thrust at about 10 km depth (Sulstarova et al., 2000; Ballauri et al., 2002), in excellent agreement with seismicity concentration at this depth found during our study (Fig.2b). Fewer than 30 events were located in depth shallower than 1km (Fig3f), clearly associated with sites of evaporite outcropping. This correlation of very shallow seismicity with evaporites is suggested by Dahm et al., 2011, which studied very weak events ($M<1$) in depth between 60 to 120 m. According to the authors the best model of ground displacement indicated that the event centroids were above the top of an old diapir.

Most of seismic events are located in the northern part of the study area. These events show a lot of variations in depth as well as focal mechanism (Fig.4), indicating tectonic complexity. Two very shallow (<3 km) clusters can be identified in the northern part. One cluster located in the coastal area south of Fterra is almost vertical, slightly dipping to the west (Fig.2b) and can probably be attributed to a fault oriented NW-SE and dipping to the west (Balaurri et al., 2002). This local structure is connected to small evaporite outcrops that formed as a result of eruptions under the effect of thrust tectonics (Velaj 2001). Fterra diapir is located in the core of Fterra-Fitore anticline structure (Vilasi et al., 2009).

Another cluster is located inland, close to Zhulati, and dips to the east. This shallow seismic event distribution is consistent with the thrust fault mapped (ISPGJ-IGJN, 1983) in the Zhulati area, which is also related to evaporites. Several seismic events in the northern part of the study area appear at depths below 3 km, whereas the main body of the events is located between 5 and 10 km depth, without any obvious dip direction. Most of the focal mechanisms are reverse type (Fig.4), suggesting that the events are mostly related to thrust faults, which is consistent with the active tectonics in the area (Cagnetti et al., 1978). Some strike-slip focal mechanisms indicate small strike-slip faults acting as transfer faults.

In the Saranda area, seismicity forms two very shallow clusters. This area is part of an anticline chain (Shendelli-Saranda-Ksamil), which gradually dips into Quaternary deposits of the Butrinti area (Meco and Aliaj, 2000). The Saranda anticline is the

outermost fold of the southern external Albanides, and is oriented NNW-SSE (Lacombe et al., 2009). It constitutes a pop-up fold, bounded by two major conjugate faults (Vilasi, 2009). The western part of the anticline forms the southern coastal area, where events are distributed almost vertically in depth, showing a slight dip to the east (Fig.2b). Focal mechanisms (Fig.4) indicate thrust and strike-slip faults in the area. According to Aliaj (2007), the thrust faults are cut by strike-slip faults, trending NE and SE.

To the southwest, the Butrinti region has a complicated geological structure with the development of diapiric processes (Hallaci and Durmishi, 2002). The Butrinti – Sagiada fault zone has generated moderate earthquakes in the past, while strong earthquakes with Mmax>6.0 are expected in the future (Aliaj, 1979). Nevertheless, during the study period, significant seismic activity was not recorded; moreover, the calculated focal mechanisms do not demonstrate any coherence (Fig.4). The lack of data is probably due to the fact that the Butrinti region is located out of the limits of the study area.

In the central part of the study area, close to Delvina, a cluster of events appears at depth below 10 km (Fig.2b). Delvina is a seismically active area, since the Delvina fault has generated many earthquakes of M>5 during the past decades (Aliaj, 1979). Moreover, in this area the evaporites of the Ionian zone, the thickness of which reaches up to 4 km, crop out along local structures (Velaj, 2001). According to Velasi (2009), the evaporites were forced to move towards lower pressure gradients when the normal faults were reactivated as thrust or strike-slip faults. The seismicity distribution in the cross section (Fig.2b) shows a gap in the central part between approximately 5 and 9 km depth. The

absence of seismicity at this depth coincides with the existence of the evaporite body close to surface. The calculated focal mechanisms indicate strike-slip and thrust faults. To the east, a smaller cluster appears in the Kronjia area, the few focal mechanisms of which indicate thrust faulting. This shallow cluster is considered to be related to the evaporite outcrop and the minor thrust faults in the area.

South of Delvina, in Cerkavica, a small cluster of shallow seismic events exists. The distribution of the events in depth between 5 and 9 km indicates a SE-dipping fault. The focal mechanisms (Fig.4) are mainly reverse and point to the thrust faults, which are mapped in the neighboring area.

2. Stress distribution

Paleostress analysis in the External Albanides by Kilias et al. (2001) indicates a NE-SW-oriented subhorizontal maximum stress axis (σ_1) and a subvertical minimum stress axis (σ_3). The deformation has been well dated as an Eocene-Early Oligocene compressional event (Collaku and Cadet, 1991). During a study of stress regime in a broader area Cagnetti et al., 1978 suggested that in Albania compressive stress is oriented NE-SW. According to this study the genesis of the earthquakes is due to horizontal compressive stresses, roughly perpendicular to the seismic and tectonic lines. Moreover, Sulstarova et al., 2000 studied focal mechanisms in SSW Albania and concluded that the causative faults were transpresional strike-slip type. The goal of this section is to determine the

stress field within the study area, which is defined by the directions of the principal stress axes.

The stress inversion method of Gephart and Forsyth (1984) is applied to calculate stress orientations from earthquake fault-plane solutions. The method is based on three basic assumptions: it is assumed that the deviatoric stress tensor is uniform over a certain region and over the time interval considered; the method assumes that earthquakes are shear dislocations on pre-existing faults; and that slip occurs in the direction of the resolved shear stress on the fault plane (Gephart, 1990).

The 810 reliable focal mechanisms indicate a complex tectonic stress field where both thrust and strike-slip faulting occur in vicinal areas (Fig.4). The stress inversion was carried out using the Zmap software (Wiemer and Zuniga, 1994) to calculate the directions of the principal stress axes σ_1, σ_2, σ_3 ($\sigma_1 \geq \sigma_2 \geq \sigma_3$) and the shape factor R ($R=(\sigma_2-\sigma_1)/(\sigma_3-\sigma_1)$, which indicates the magnitude of σ_2 relative to σ_1 and σ_3. The best-fitting stress is achieved when the misfit between the values computed from the stress tensor and the observed fault plane and slip direction reach a minimum on each plane of the focal mechanism (Gephart and Forsyth, 1984). This misfit is calculated through a grid search, systematically varying the orientation of the principal stresses and the parameter R. The stress tensor that corresponds to the minimum average rotation angle is assumed to be the best stress tensor for the specific population of focal mechanisms (Kiratzi, 1999).

Since both strike-slip and reverse type focal mechanisms exist in neighboring areas, heterogeneity in the stress regime is possible; thus, the dataset must be subdivided during the stress inversion according to the spatial distribution of the seismic events. Six areas were defined within the study area, which are orientated NNW-SSE, parallel to the tectonic structures: a) the northern part of the study area (N), which includes a large portion of the seismicity, b) the northwestern part (NW), which covers the northern coast of the study area, c) the western–coastal area (W), which includes the Saranda clusters, d) the central part (C), including the Delvina cluster, e) the eastern part of the study area (E), which contains several spread events and f) the southern part (S), including the Cerkovica cluster. The results are summarized in Table 2 and Figure 5.

The stress inversion for the northern part (N) of the study area reveals that the area is under compression of NNE-SSW direction. The central part (C) of the study area (Delvina) and the eastern part (E) also indicate compression. These three areas (Fig. 6) are bounded to the west and east by two large thrust faults, which cross the southern Albania in a NNW-SSE direction.

The stress regime derived from these results (Fig.6) is consistent with the major faults of the area and the stress descriptions in previous studies (Sulstarova et al., 2000; Ballauri et al., 2002). Focal mechanisms in Albania studied by Cagnetti et al. (1978) reveal that most of the earthquake solutions were reverse-slip type, while tensional were few. In general, they suggest compressional stress with a NNE–SSW azimuth, which may be considered as the principal agent causing the earthquakes (Cagnetti et al., 1978).

The stress inversion results for the coastal part of the study area, which includes the northwestern part (NW) and the Saranda–Ksamil western coast (W), reveal strike-slip faulting type. This indicates that the shallow seismicity, which is concentrated in clusters in the coastal area of southern Albania, can be attributed to the activation of minor transfer faults. The existence of transfer faults is also supported by the tomographic results (Tselentis et al., 2011), which indicate that large parts of the anticlines, along the coastal area, are shifted. Further south, at the edge of the study area (S), the results also indicate strike-slip faulting. These results suggest the coexistence of compressional and transpressional movements in the coastal area. In the Saranda area, the paleostress analysis by Lacombe et al. (2009) recorded a true NE-SW compression (σ_3 vertical) and a subperpendicular extension rather related to a strike-slip stress regime. This may reflect a local inhomogeneity of the stress regime through time (Lacombe et al., 2009). The existence of strike-slip faulting in the area agrees with the tectonic regime suggested by Tselentis et al. (2006) in the neighboring northwestern Greece.

Conclusions

During a dense temporary seismic network installation in the southernmost Albania, 2113 events were detected. The distribution of the epicenters provides a complete image of the seismic activity in southernmost Albania. The seismic events are concentrated mainly in clusters indicating active faults in the area. The seismicity is rather shallow, concentrated to the upper 10km of the crust and is slightly dipping to the East, which is in agreement

with seismic profile imaging the sole thrust at about 10 km depth (Sulstarova et al., 2000; Ballauri et al., 2002).The shallower seismicity clusters in Fterra, Zhulati and Kronja (Fig3a) are local structures connected to small evaporite outcrops that formed under the effect of thrust tectonics (Velaj, 2001).

The fault plane solutions of 810 events were determined using a high quality dataset. Reverse focal mechanisms prevail, while a considerable number of strike slip focal mechanisms also exist and oblique focal mechanisms were rare. The results confirm the existence of NE-SW thrusts occasionally interrupted by NE-SW strike-slip faults (Tiberti et al., 2008). Available focal solutions show NE-SW compression at shallow depth, consistent with the geometry of the thrusts detected in seismic profiles (Piccinini et al., 2006). The stress analysis revealed the existence of pure compressional but also transpressional stress regimes, both having NE-SW direction. In detail, a small change in the stress setting from pure thrust to transpression is observed from the central area (Kurveleshi belt) towards the coastal area (Cika belt) (Fig.6). Further more, an attempt to resolve stress tensor changes with depth revealed that the stress regime is stable in the vertical direction.

Compressional stress is indicated by the transposition of the surface and shallow formations, mainly to the west, by thrust faults. In some cases the faulting seems to be connected to the evaporite outcropping. The shift of parts of the anticline, in the western zone, indicates transfer faulting. The major faults are imaged clearly by the seismicity and the stress regime is mapped.

The mainly shallow seismicity distribution, the occurrence of evaporites and the coexistence of compressional and transpressional stress regime found in Southwestern Albania are in excellent agreement with the results obtained for the area of the Epirus of Northwestern Greece (Tselentis et al. 2006). Thus we may assume that the geotectonic environments are similar for these two areas, which is useful for a seismic hazard survey or an oil exploration study of the broader area of Adriatic.

Data and Resources

The seismological data that were used in this study were collected during a Passive Seismic Tomography Survey in the scope of Hydrocarbon Exploration. The project has been assigned to Landtech Enterprises S.A by Stream Oil & Gas Ltd.

Acknowledgments

We would like to thank Stream Oil & Gas Ltd for the permission to use the seismological data.

References

Albania Ministry of Industry and Energy. (2003). Final Environmental Impact Assessment–Vlorë Combined, Project#1003316.013901.

Aliaj Sh (1979). Sizmotektonika dhe Kriteret Gjeologjike te Sizmicitetit te Shqiperise, *Candidate of Science Thesis*, Archive of Seismological Institute, Tirana, 251 pp.

Aliaj Sh., (2007). Seismogenic Models for Albania: Overview of Relevant Data. *First Workshop for the NATO Science for Peace,* Project NO. 983054, "Harmonization of Seismic Hazard Maps for the Western Balkan Countries", Ig near Ljubljana, Slovenia, 7 –9 November.

Ballauri, A., Bega, Z., Meehan, P., Gambini, R., and Klammer, W. (2002), Exploring in structurally complex thrust belt: Southwest Albania Case, *AAPG Hedberg Conference*, May 14-18, 2002, Palermo-Mondello (Sicily, Italy).

Cagnetti, V., V. Pasquale and S. Polinari, (1978). Fault-plane solutions and stress regime in Italy and adjacent regions, *Tectonophysics* **46**, 239–250.

Collaku, A. and Cadet, J.P., (1991). Sur l allochtonie des Albanides: apport des donnees de l' Albanie septentrionale, *Bul. Shk, Gjeol,* **1**, 255–270.

Dahm, Torsten; Heimann, Sebastian; Bialowons, Wilhelm. (2011). *Natural Hazards*, 5**8**, **3**, 1111-1134.

Evans J.R., D. Eberhart-Phillips and C.H. Thurber, (1994). User's manual for SIMULPS12 for imaging Vp and Vp/Vs: A derivative of the Thurber tomographic inversion SIMUL3 for Local Earthquakes and Explosions. U.S. Geological Survey, *Open File Report*, 94–431.

Gephart, J.W and D.W. Forsyth (1984). An improved method for determining the regional stress tensor using earthquake focal mechanism: application to the San Fernando earthquake sequence, *J. Geophys. Res.*, **89**, 9305-9320.

Gephart, J (1990) Stress and the direction of slip on fault planes, *Tectonics*, **9**, 845 858.

ISPGJ-IGJN (1983). Geological map of Albania. Tirana, Albania. Scale 1:200,000.

ISPGJ-IGJN (1985). Geological map of Albania. Tirana, Albania. Scale 1:200,000.

Kilias A., M. Tranos, D. Mountrakis, M. Shallo, A. Marto, I. Turku (2001). Geometry and kinematics of deformation in the Albanian orogenic belt during the Tertiary, *Journal of Geodynamics*, **31, 2**, 169-187.

Kiratzi, A., (1999). Stress tensor inversion in Western Greece using earthquake focal mechanisms from the Kozani–Grevena 1995 seismic sequence, *Ann. Geophys.,* **42**, 725 – 734.

Kissling, E., W. L. Elsworth, D. Eberhart-Phillips, and U. Kradofler (1994). Initial reference models in seismic tomography*, J. Geophys. Res*. **99**, 19,635–19,646.

Korn, G. and T. Korn, (1968) Mathematical Handbook for Scientists and Engineers *McGraw-Hill Book Company*, New York.

Lacombe, O., J.,Malandain, N., Vilasi, K., Amrouch, F., Roure, (2009). From paleostresses to paleoburial in fold–thrust belts: Preliminary results from calcite twin analysis in the Outer Albanides *Tectonophysics*, **475**, Issue 1, Pages 128-141.

Lee, W.H.K. and J.C. Lahr (1975). HYPO71 (Revised): A Computer Program for Determining Hypocenter, Magnitude, and First Motion Pattern of Local Earthquakes, *U.S. Geol. Surv. Open File Rept. OF* 85-749.

Lee W.H.K. and C.M. Valdes (1985). HYPO71PC A personal computer version of the HYPO71 earthquake location program, *U.S.Geol. Surv. Open-File Rept. OF* 85-749

Luan Nikolla, Vlasta Tari-Kovacic & Arso Putnikovic, (2002). Stratigraphy and evolution of Ionian foreland basin. Exploration methods in highly explored basins. ***3rd*** *International Symposium on Petroleum Geology*, Zagreb, CROATIA. 79-83.

Meco, S. and Aliaj, S., (2000). Geology of Albania. *Borntraeger Science Publishers*, Stuttgart. pp 246.

Muco B., Vaccari F., Panza G., N. Kuka.(2002. Seismic zonation in Albania using a deterministic approach, *Tectonophysics,* **344**, 277– 288.

National Agency of Natural Resources. (2007). Natural Resources in Albania, Report, Tirana, 2007, pp29.

Papazachos, B., and Papazachou, C., (1997). The earthquakes of Greece. *Ziti Editions*, Thessaloniki, Greece.

Piccinini, D., Chiarabba, C., Augliera, P., and Monghidoro Earthquake Group (M.E.G.) (2006), Compression along the northern Apennines? Evidence from the Mw 5.3 Monghidoro earthquake, *Terra Nova* **18**, 89–94.

Reasenberg, P. and D. Oppenheimer (1985). FPFIT, FPPLOT and FPPAGE: Fortran Computer Programs for Calculating and Displaying Earthquake Fault Plane Solutions, *U. S. Geol. Surv. Open-File Rept. OF 95-515,* pp 24.

Robertson A. and M. Shallo (2000). Mesozoic-Tertiary tectonic evolution of Albania in its regional Eastern Mediterranean context, *Tectonophysics*, **316**, 3-4,

Robertson, A., J. Overpeck, D. Rind, E. Mosley-Thompson, G. Zielinski, J. Lean, D. Koch, J. Penner, I. Tegen, and R. Healy, (2001). Hypothesized climate forcing time series for the last 500 years. *J. Geophys. Res.*, **106**, 14783-14803

Sulstarova, E., Peçi, V., and Shuteriqi, P. (2000), Vlora-Elbasani-Dibra (Albania) transversal fault zone and its seismic activity, *Journal of Seismology* **4**, 117–131.

Tselentis, G-A., E. Sokos, N. Martakis and A. Serpetsidaki., (2006). Seismicity and Seismotectonics in Epirus, Western Greece: Results from a Microearthquake Survey. *Bulletin of the Seismological Society of America*, **96**, No. 5, 1706–1717.

Tselentis, G-A., N. Martakis, P. Paraskevopoulos and A. Lois, (2011). High resolution passive seismic tomography for 3D velocity, Poisson and Qp structure at Delvina hydrocarbon field - S. Albania *Submitted to Geophysics*.

Tiberti, M. M., Lorito, S., Basili, R., Kastelic, V., Piatanesi A. and G. Valensise (2008) Scenarios of earthquake generated tsunamis in the Adriatic Sea. *PAGEOPH,* **165**, **11-12,** 2117-2142.

Thurber, C. H. (1986). Analysis methods for kinematic data from local earthquakes, *Rev. Geophys.* **24,** 793–805.

U.S. Geol. Surv. (USGS) National Earthquake Information Center, World Data Center A for Seismology, *http://wwwneic.cr.usgs.gov*.

Velaj, T., 1985. Evaporit tectonic role in determination of the Ionian tectonic zone physionomy: *Oil an Gas Bulletin*, 17-38.

Velaj, T., (2001). Evaporites in Albania and their impact on the thrusting processes. *Journal of the Balkan Geophysical Society*, **4**, 9-18.

Vilasi, N., Malandain, J., Barrier, L., Callot, J.-P., Amrouch, K., Guilhaumou, N., Lacombe, O., Muska, K., Roure, F., Swennen, R. (2009). From outcrop and petrographic studies to basin-scaale fluid flow modelling: the use of the Albanian natural laboratory for carbonate reservoir characterization, *Tectonophysics,* **474**, 367-392.

Wiemer, S. and F. R. Zuniga, (1994). ZMAP - a software package to analyze seismicity. EOS, Transactions*, Fall Meeting, AGU*, **75**, 456.

Xanalatos, N., and G-A. Tselentis (1997). SEISMWIN, an algorithm for processing seismological waveforms. *Proc. Geol. Soc. Athens,* **22,** 235–246.

Tables

Table1. The 1-D velocity model used in earthquake location

Depth (km)	Vp (km/s)
0.00	5.12
2.00	5.33
4.00	5.52
6.00	5.62
8.00	5.82
10.00	6.05
15.00	6.25
20.00	6.39
30.00	6.50
40.00	8.00

Table2 The stress parameters derived for different regions of the study area.

Region		Type	σ_1	σ_2	σ_3	R	Misfit
Northern	(N)	Thrust	30/233	19/334	53/91	0.6	5.50
Northwestern	(NW)	Strike-Slip	11/221	54/115	34/318	0.8	0.62
Western-coastal	(W)	Strike-Slip	9/254	80/86	2/345	0.3	7.00
Central	(C)	Thrust	32/72	11/169	56/276	0.9	7.00
Eastern	(E)	Thrust	3/62	5/152	84/297	0.6	8.00
Southern	(S)	Strike-Slip	13/80	66/319	20/174	0.8	6.50

Figure Captions

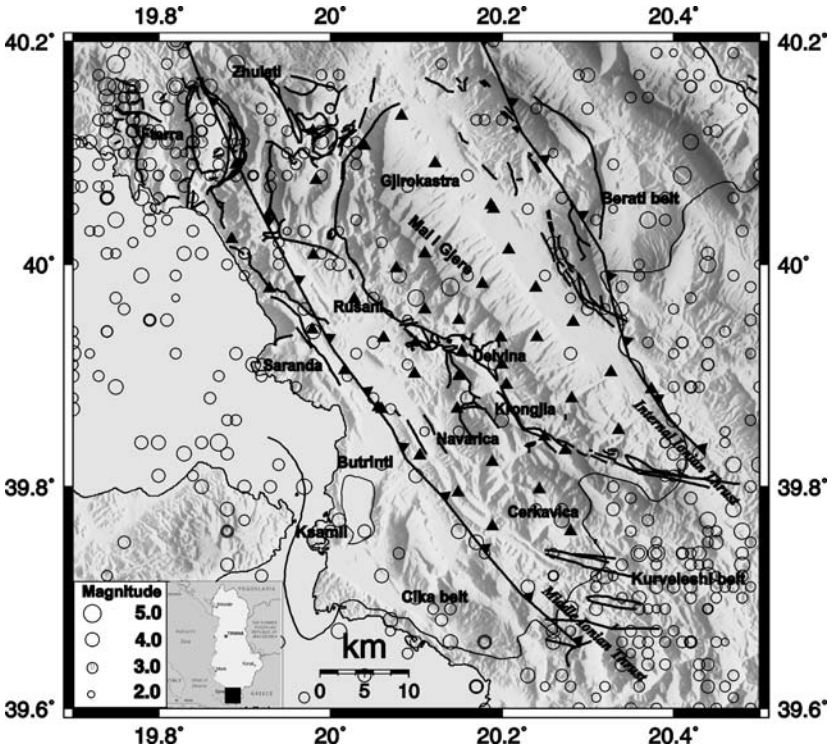

Figure 1. Map of the main tectonic structures (Robertson and Shallo, 2000; ISPGJ-IGJN, 1985) and seismicity during the period 1973-2008 (USGS catalog). The black triangles represent the seismological stations installed during the experiment.

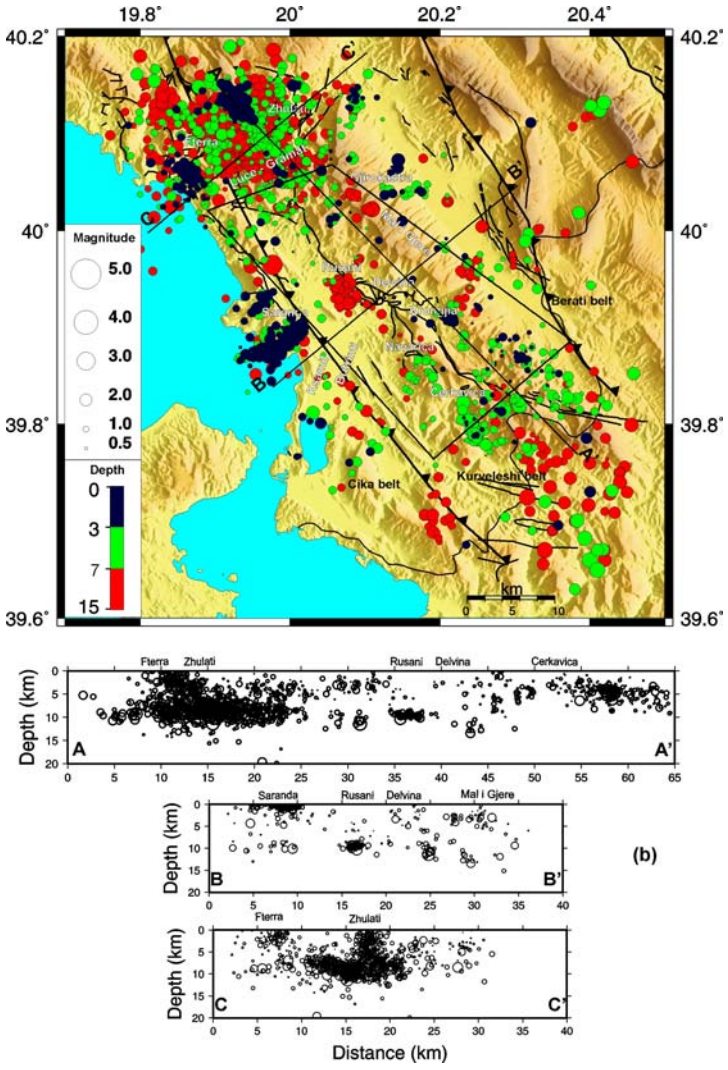

Figure 2. a) Seismicity map of the 2113 events that were located in this study. b) seismicity cross-sections across the study area. Fault lines are taken from ISPGJ-IGJN (1983, 1985).

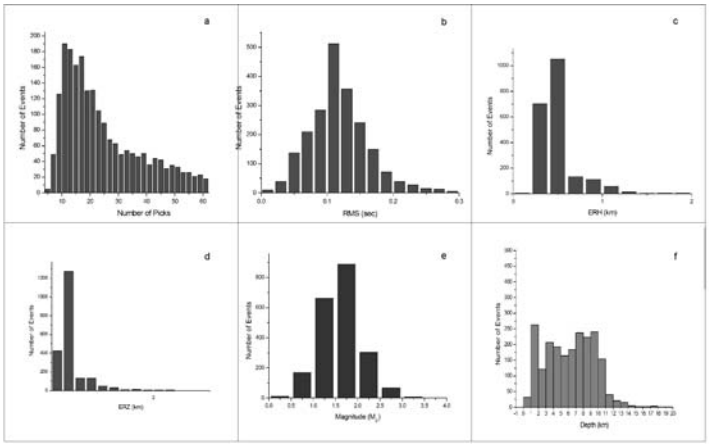

Figure 3. Histogram of a) the number of P and S first arrival picks. b) RMS arrival time residuals in seconds. c) ERH horizontal error in km. d) Histogram of the ERZ vertical error in km. e) duration Magnitude. f) depth in km.

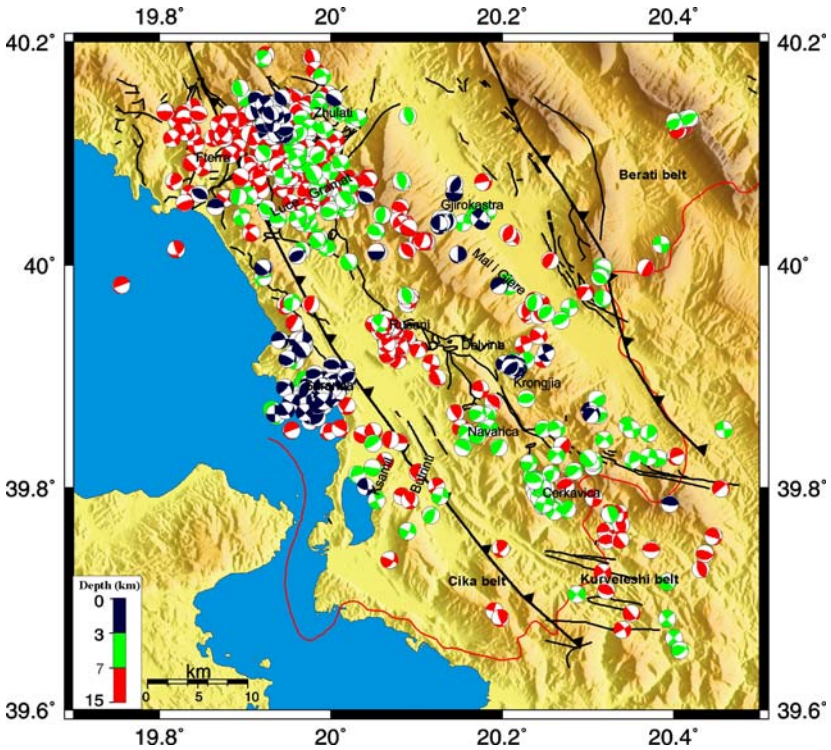

Figure 4. Map of the unique fault plane solutions for 810 events (lower hemisphere projection, compressive quadrant shaded).

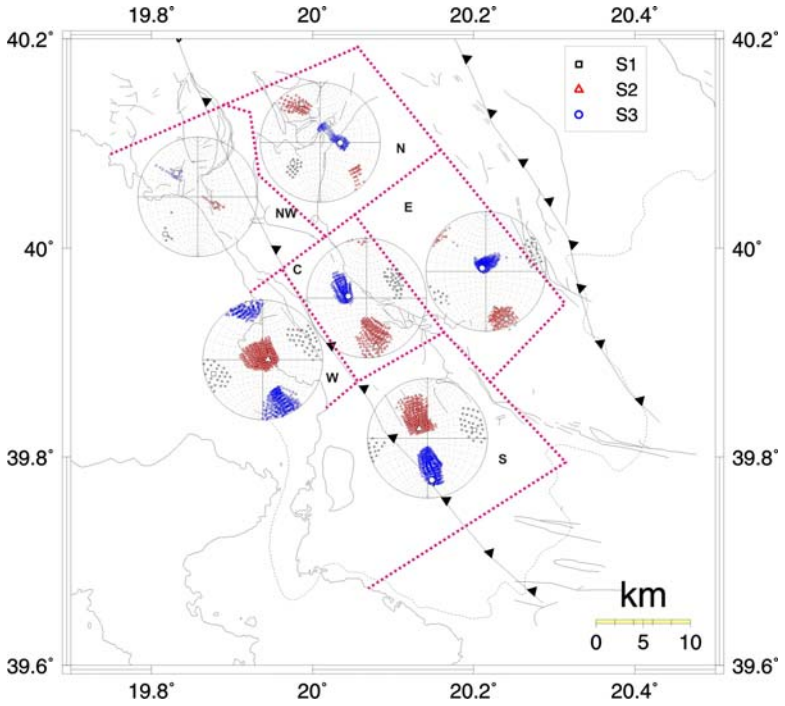

Figure 5. Stress tensor inversion results for six regions within the study area.

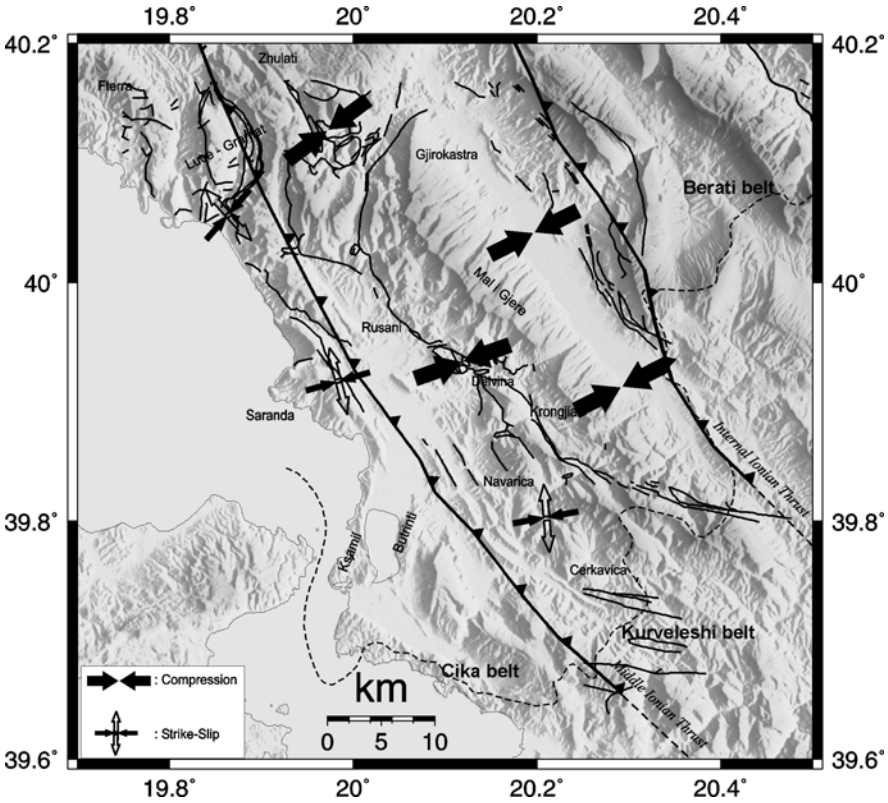

Figure 6. Stress axis orientations derived during this study